Med Chem Res (2013) 22:4877–4885
DOI 10.1007/s00044-013-0497-4

MEDICINAL CHEMISTRY RESEARCH

ORIGINAL RESEARCH

# Steroidal saponins from the leaves of *Yucca de-smetiana* and their in vitro antitumor activity: structure activity relationships through a molecular modeling approach

**Jacqueline Eskander · Ola K. Sakka · Dominique Harakat · Catherine Lavaud**

Received: 2 October 2012 / Accepted: 15 January 2013 / Published online: 30 January 2013


**Abstract** Four steroidal saponins were isolated from the leaves of *Yucca de-smetiana* Baker. Their structures were established using one- and two- dimensional NMR spectroscopy and mass spectrometry. The structure of the new steroidal saponin was identified as: (25*R*)-3β-hydroxy-5 α-spirostan-3-*O*-β-D-xylopyranosyl-(1 → 2)-β-D-galactopyranosyl-(1 → 2)-*O*-[β-D-glucopyranosyl-(1 → 3)]-β-D-glucopyranosyl-(1 → 4)-β-D-galactopyranoside (desmettianoside C) along with three known spirostanol and furostanol saponins. The isolated saponins were evaluated for their antitumor activity against HCT116, MCF7, HepG2, and A549 cell lines. Saponins **3** and **4** showed potent activity against HCT116, MCF7, and HepG2 cell lines in comparison with the positive control doxorubicin. A molecular modeling approach was performed to establish conformational criteria that could affect the biological activity of the isolated saponins.

J. Eskander (✉) · C. Lavaud
Laboratoire de Pharmacognosie, Institut de Chimie Moléculaire de Reims (ICMR), UMR-CNRS 7312, Bâtiment 18, BP 1039, 51687 Reims Cedex 2, France
e-mail: Jacqueline.eskander@hotmail.com

O. K. Sakka
Department of Chemistry, American University in Cairo, P.O. Box 74, New Cairo 11835, Egypt

D. Harakat
Service d'analyse, Institut de Chimie Moléculaire de Reims (ICMR), UMR-CNRS 7312, Bâtiment 18, BP 1039, 51687 Reims Cedex 2, France

*Present Address:*
J. Eskander
Pharmacognosy Department, Faculty of Pharmacy, Helwan University, POB 11795, Ain-Helwan, Cairo, Egypt

**Keywords** *Yucca de-smetiana* · Steroidal saponins · Desmettianoside C · Antitumor activity · Molecular modeling

## Introduction

*Yucca* genus (Agavaceae) is widely distributed in central and northern America; many of them are cultivated in the tropical gardens of the world as ornamental plants. The main application of *Yucca* products is in animal nutrition as a food additive to reduce ammonia and fecal odors in animal excreta (Cheeke, 2000) and improve the growth and productivity of livestock and poultry (Anthony *et al.*, 1994; Balog *et al.*, 1994). Another important application for *Yucca* extracts is as a foaming agent in soft drink, pharmaceutical, cosmetic, and food industries, which is attributed to the very high steroidal saponins content in *Yucca* species (Piacente *et al.*, 2005; Oleszek *et al.*, 2001; Hostettmann and Marston, 1995; Mahato *et al.*, 1982). Studies of steroidal saponins from *Yucca* genus have mainly focused on *Y. schidigera* (Oleszek *et al.*, 2001), *Y. gloriosa* (Skhirtladze *et al.*, 2006), *Y. filamentosa* (Dragalin and Kintia, 1975), *Y. elephantipes* (Zhang *et al.*, 2008), *Y. aloifolia* (Bahuguna and Sati, 1990), and *Y. smalliana* (Jin *et al.*, 2007). Some of these species showed antifungal (Jin *et al.*, 2007), antibacterial, antiprotozoal, hypocholesterolemic (Piacente *et al.*, 2005), and antitumor (Balestrieri *et al.*, 2006; Ali *et al.*, 1978) activities. As part of our chemical investigations on steroidal saponins of medicinal values (Eskander *et al.*, 2010, 2011), we studied the leaves of *Y. de-smetiana* Baker cultivated in Egypt. Recently, two furostanol saponins named desmettianosides A and B were isolated from the aqueous methanolic extract of the same source which was incorrectly

worded *Y. desmettiana*; these compounds exhibited high molluscicidal activity (Diab *et al.*, 2012). In addition, this paper reports the isolation and structural elucidation of four steroidal saponins from
*Y. de-smetiana*, among which, one is a new compound named desmettianoside C. The antitumor activities of saponins **1**–**4** were evaluated against HCT116 (colon), MCF7 (breast), HepG2 (hepatoma), and A549 (lung) cell lines in an attempt to discover new antitumor compounds. Secondly, a comprehensive structural activity relationship (SAR) was performed using conformational analysis, construction of hydrophobic and hydrophilic bonding mappings, rigid and flexible alignment to infer a relationship between the cytotoxicity of our isolated saponins and their structures.

## Results and discussion

The leaves of *Y. de-smetiana* were extracted with MeOH to give a crude extract which was precipitated by acetone. The saponin mixture was obtained after removal of saccharides by passing the precipitate through a porous gel polymer column (Diaion HP-20). The fractions containing saponins were purified using combination of reversed-phase $C_{18}$ column, silica gel column chromatography, and preparative TLC to afford four saponins (**1**–**4**) (Fig. 1). Three known compounds (**1**–**3**) were identified the structural assignments of which were made by analysis of ESI–MS and 2D- NMR spectral data including COSY, TOCSY, HSQC, HMBC, and ROESY. Characterization was carried out by comparison of their data with those reported in literature.

Saponin **1** with a high-resolution ESI–$MS^+$ $[M + Na]^+$ at *m/z* 943.4885 (calc. 943.4879, $C_{45}H_{76}O_{19}Na$) was identified as (25*R*)-26-*O*-β-D-glucopyranosyl-5β-furostan-3β,22α,26-triol 3-*O*- [β-D-glucopyranosyl-(1 → 2)-*O*-β-D-galactopyranoside], previously isolated from *Y. gloriosa* (Skhirtladze *et al.*, 2006) and *Y. elephantipes* (Zhang *et al.*, 2008).

Saponin **2** with a high-resolution ESI–$MS^+$ $[M + Na]^+$ at *m/z* 957.5025 (calc. 957.5035, $C_{46}H_{78}O_{19}Na$) was established as (25*R*)-26-*O*-β-D-glucopyranosyl-22α-methoxy-5β-furostan-3β, 26-diol 3-*O*-[β-D-glucopyranosyl-(1 → 2)-*O*-β-D-galactopyranoside], previously isolated from *Y. gloriosa* (Skhirtladze *et al.*, 2006).

Saponin **3** with a high-resolution ESI–$MS^+$ $[M + Na]^+$ at *m/z* 763.4250 (calc. 763.4245, $C_{39}H_{64}O_{13}Na$) was assigned to smilagenin 3-*O*-[β-D-glucopyranosyl-(1 → 2)-*O*-β-D-galactopyranoside], previously isolated from *Y. gloriosa* (Nakano *et al.*, 1989) and *Y. elephantipes* (Zhang *et al.*, 2008).

Saponin **4**, isolated as an amorphous solid, showed an accurate $[M + Na]^+$ ion at *m/z* 1219.5735 in the positive HR-ESI–MS, corresponding to the empirical molecular formula $C_{56}H_{92}O_{27}Na$. The $^1H$ NMR spectrum displayed signals for two tertiary methyl groups at δ 0.61 (s), 0.80 (s) and two secondary methyl groups at δ 0.67 (d, $J = 5.6$ Hz), 1.12 (d, $J = 7.0$ Hz). On the basis of the HSQC and HMBC correlations, the aglycone moiety was identified as (25*R*)-5α- spirostan-3β-ol known as tigogenin (Agrawal *et al.*, 1985) previously isolated from *Yucca* species (Mahato *et al.*, 1982). The C-25 configuration was deduced to be (*R*) based on the difference in chemical shifts of the geminal protons $CH_2$-26 ($\Delta\delta_H = 0.09$ ppm). It has been established that $\Delta\delta_H$ is <0.1 ppm in 25*R*- spirostane steroids, whereas $\Delta\delta_H$ 0.63–0.79 ppm confirmed the 25*S*- configuration (Agrawal, 2003). The ROE correlation observed between H-26ax at δ 3.58 and Me-27 at δ 0.67 confirmed the 25*R*- configuration. The ROE correlations between H-1α (ax) and H-3, H-3 and H-5 provided evidence of the β-configuration of C-3 oxygen atom and the α-configuration of H-5.

The analysis of the saccharide part of **4** was deduced by the observation of five anomeric proton signals at δ 4.86 (d, $J = 7.8$ Hz), 5.09 (d, $J = 7.4$ Hz), 5.13 (d, $J = 7.9$ Hz), 5.20 (d, $J = 7.8$ Hz), and 5.55 (d, $J = 6.8$ Hz) in the $^1H$ NMR spectrum associated with five anomeric carbons resonating at $\delta_C$ 102.2, 105.9, 104.6, 104.3, and 103.8, respectively, through the HSQC experiment. The nature of monosaccharides was identified as D-galactose, D-glucose, and D-xylose from acid hydrolysis of saponin mixture. Complete assignment of the glycosidic protons was achieved by analysis of the COSY and TOCSY experiments, while those of the corresponding glycosidic carbons were determined through the direct H–C correlations in the HSQC spectrum. The anomeric signals at δ 4.86 (d, $J = 7.8$ Hz) and 5.55 (d, $J = 6.8$ Hz) were identified as two β-D-galactopyranosyl units from their characteristic equatorial H-4 δ 4.58 (dd, $J = 4.0$, 2.6 Hz) and 4.04 (d, $J = 2.5$ Hz). The signals at δ 5.13 (d, $J = 7.9$ Hz) and 5.20 (d, $J = 7.8$ Hz) belonged to the typical spins systems of β-D-glucopyranosyl moieties with their H-1 to H-5 in axial positions ($^3J_{H-H} > 7.0$ Hz). The last anomeric proton signal at δ 5.09 (d, $J = 7.4$ Hz) was identified as β-D-xylopyranosyl unit. The large $^3J_{H\text{-}1,\ H\text{-}2}$ coupling constant for those five sugar units indicated the β- anomeric configuration. Glycosidation shifts were observed for C-4 $_{gal}$ (δ 79.7), C-2 $_{glc'}$ (δ 80.6), C-3 $_{glc'}$ (δ 88.3), and C-2 $_{gal'}$ (δ 86.6). The linkage of the sugar units and their sequencing were confirmed using the HMBC spectrum, which showed key correlation peaks between the proton signal at δ 4.86 (H-$1_{gal}$) and (δ 77.3) C-3 of the aglycone, 5.13 (H-$1_{glc'}$) and (δ 79.7) C-$4_{gal}$, 5.20 (H-$1_{glc''}$) and (δ 88.3) C-$3_{glc'}$, 5.55 (H-$1_{gal'}$) and (δ 80.6) C-$2_{glc'}$, 5.09 (H-$1_{xyl}$) and (δ 86.6) C-$2_{gal'}$. ROEs observed across the glycosidic bonds confirmed the previous assignments of the HMBC spectrum. Thus, saponin

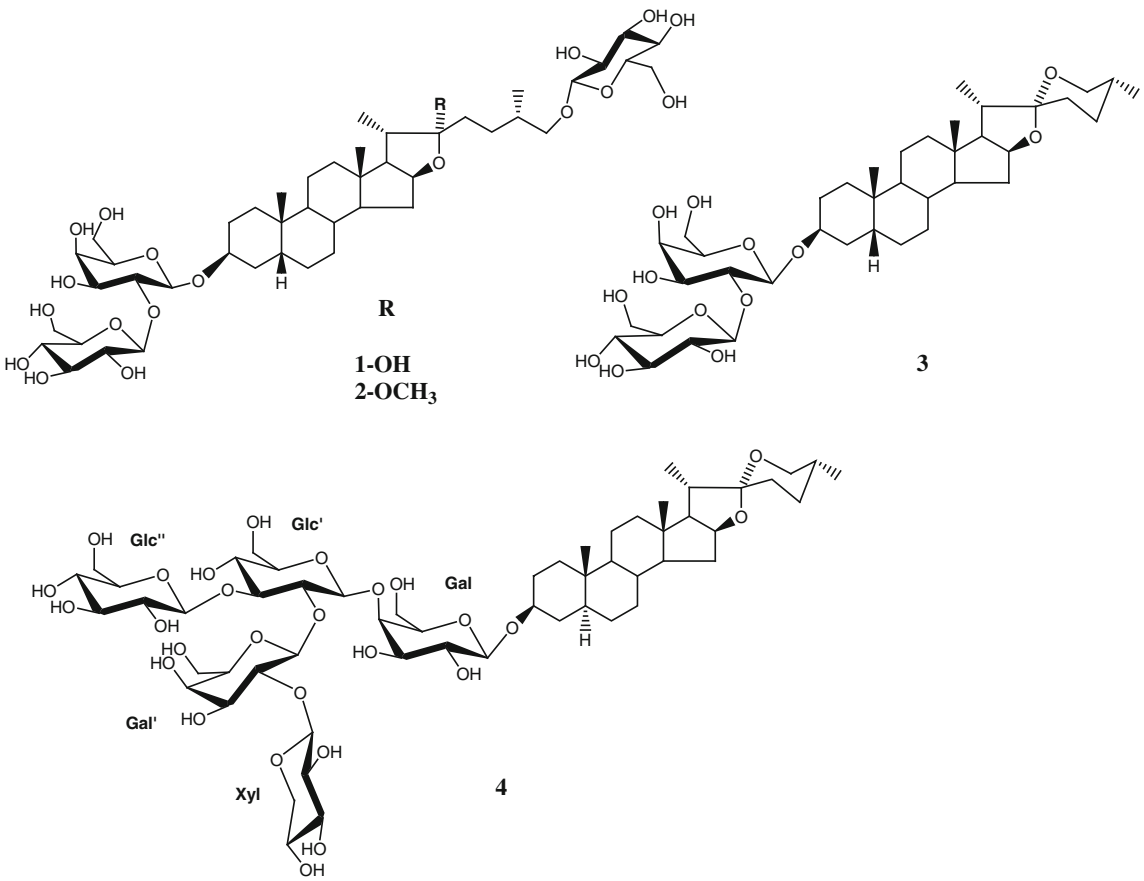


**Fig. 1** Isolated saponins (**1**–**4**) from *Yucca de-smetiana* leaves

**4** was deduced to be (25*R*)-3β-hydroxy-5α-spirostan-3-*O*-β-D-xylopyranosyl-(1 → 2)-β-D-galactopyranosyl-(1 → 2)-*O*-[β-D-glucopyranosyl-(1 → 3)]-β-D-glucopyranosyl-(1 → 4)-β-D-galactopyranoside, and named desmettianoside C.

## In vitro anti-tumor evaluation

The cytotoxic activity of saponins **1**–**4** was investigated against HCT116 (colon), MCF7 (breast), HepG2 (hepatoma), and A549 (lung) cell lines. The results are presented as the inhibitory concentration ($IC_{50}$) that inhibits the growth of cells by 50 % when compared with untreated cells after using MTT assay (Table 1). The anticancer drug Doxorubicin was also included in the study as a comparison. Furostanol saponins **1** and **2** showed no cytotoxicity against all cell lines while spirostanol saponins **3** and **4** were able to inhibit tumor cells in a dose-dependent manner (Fig. 2). Since inactive saponins **1** and **2** shared the same common β-D-glucopyranosyl-(1 → 2)-*O*-β-D-galactopyranoside sugar chain as active saponin **3**, the difference in cytotoxicity could be attributed to the presence of the spirostan aglycone. Saponin **4** showed higher potency than saponin **3** against all cell lines. Upon examination of structures of saponins **3** and **4**, we can conclude that an increase in the number of sugar moieties leads to an increase in cytotoxicity. Saponin **4** showed the highest inhibitory effect against HCT116 cells ($IC_{50}$ 2.4 μM) as compared to **3** ($IC_{50}$ 4.4 μM). Saponin **4** also showed higher potency against MCF7 cells ($IC_{50}$ 2.6 μM) than saponin **3** ($IC_{50}$ 4.0 μM) and was almost two folds more active than the positive control doxorubicin. Saponins **3** and **4** exhibited a relatively weak in vitro cytotoxic activity against A549 tumor cell line with $IC_{50}$ values of 16.5 μM and 10.2 μM, respectively, compared with the positive

**Table 1** The in vitro cytotoxicity ($IC_{50}$, μM) of isolated saponins from *Y. de-smetiana*

| Cell line | Doxorubicin | **3** | **4** |
|---|---|---|---|
| HCT116 | 6.86 | 4.4 ± 0.47 | 2.4 ± 0.57 |
| MCF7 | 5.46 | 4.0 ± 0.85 | 2.6 ± 0.49 |
| A549 | 0.84 | 16.5 ± 1.45 | 10.2 ± 0.97 |
| HepG2 | 7.36 | 3.5 ± 0.41 | 1.1 ± 0.56 |

Compounds **1**–**2** having $IC_{50}$ values larger than 100 μM are not included in the table

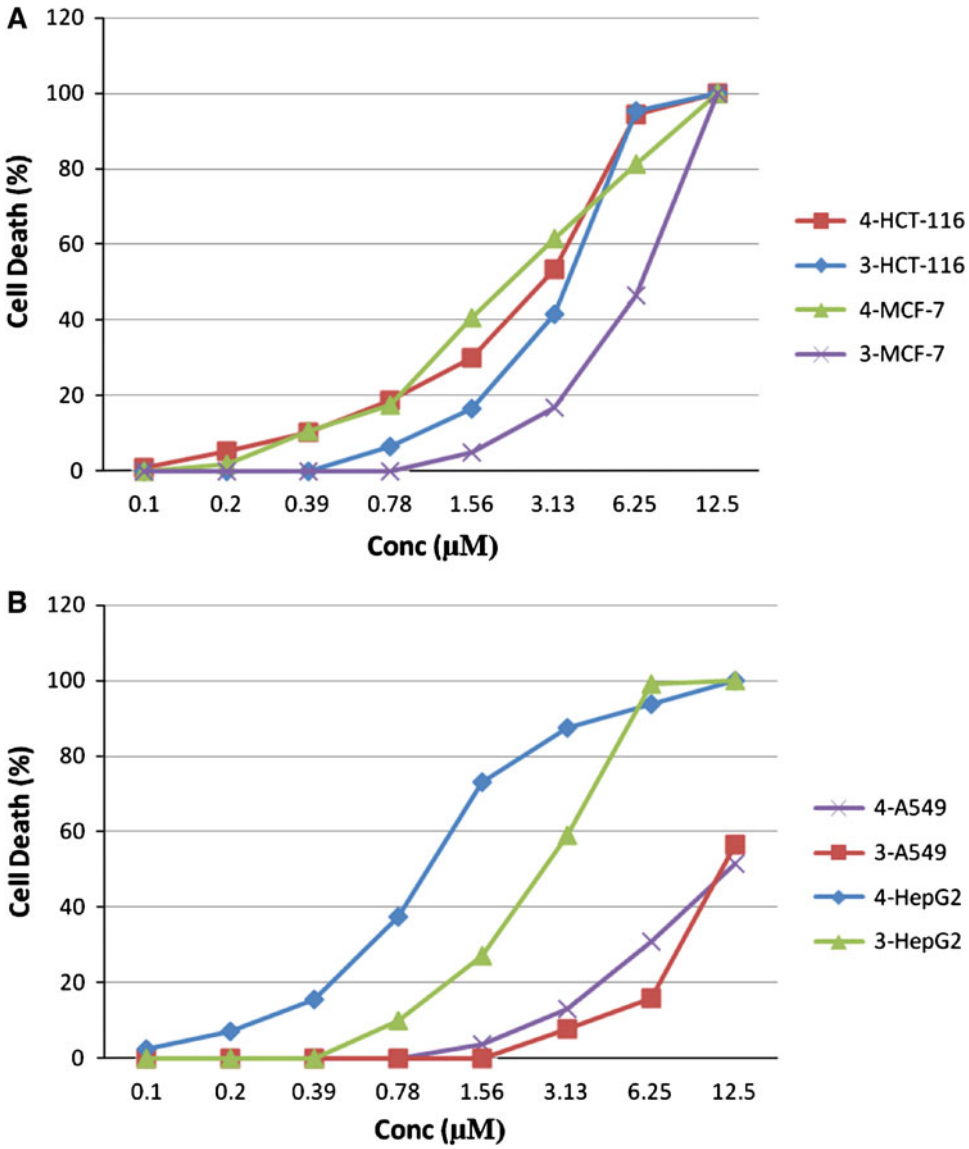


**Fig. 2** **a** The effects of saponins **3** and **4** on cell death in HCT116, MCF7 cells. **b** The effects of saponins **3** and **4** on cell death in A549 and HepG2 cells

control doxorubicin ($IC_{50}$ 0.84 µM). Desmettianoside C (**4**) showed the highest inhibitory effect against HepG2 cells ($IC_{50}$ 1.1 µM) in comparison to **3** ($IC_{50}$ 3.5 µM) while **3** was almost two folds more active than positive control doxorubicin against HepG2 tumor cell line.

## Conformational analysis

The correlation between the presence of a spirostanol structure and anticancer activity of steroidal saponins was previously reported (Yuen-Nei Cheung *et al.*, 2005; Gonzalez *et al.*, 2003, Liu *et al.*, 2004), and remarkable reports (Labrada *et al.*, 2011; Mimaki *et al.*, 2001; Trouillas *et al.*, 2005) studied conformational and electronic differences between natural and synthetic saponins possessing the spirostan aglycone. To date, limited information on the structure activity relationship (SAR) of different steroidal aglycones and their cytotoxicity is available. In this study, we report a comprehensive SAR analysis on both the spirostan and furostan aglycones existing in our isolated saponins **1**–**4** using molecular modeling to pursue information regarding their different cytotoxic activities.

The fact that both furostan saponins showed no significant cytotoxic activity against all cell lines, although disappointing, provides new information regarding important structural elements that seem to be required for cytotoxicity. Since isolated spirostanol saponin **3** shared the same common β-D-glucopyranosyl-(1 → 2)-*O*-β-D-galactopyranoside sugar chain, the difference in cytotoxicity could be attributed to the type of aglycone and to the possible existence of the sugar chain in different conformations with varying contributions to the partition function. The lowest energy-minimized structures for saponins **1**–**4** are shown in Fig. 3. To allow for a better visualization of the conformational differences between

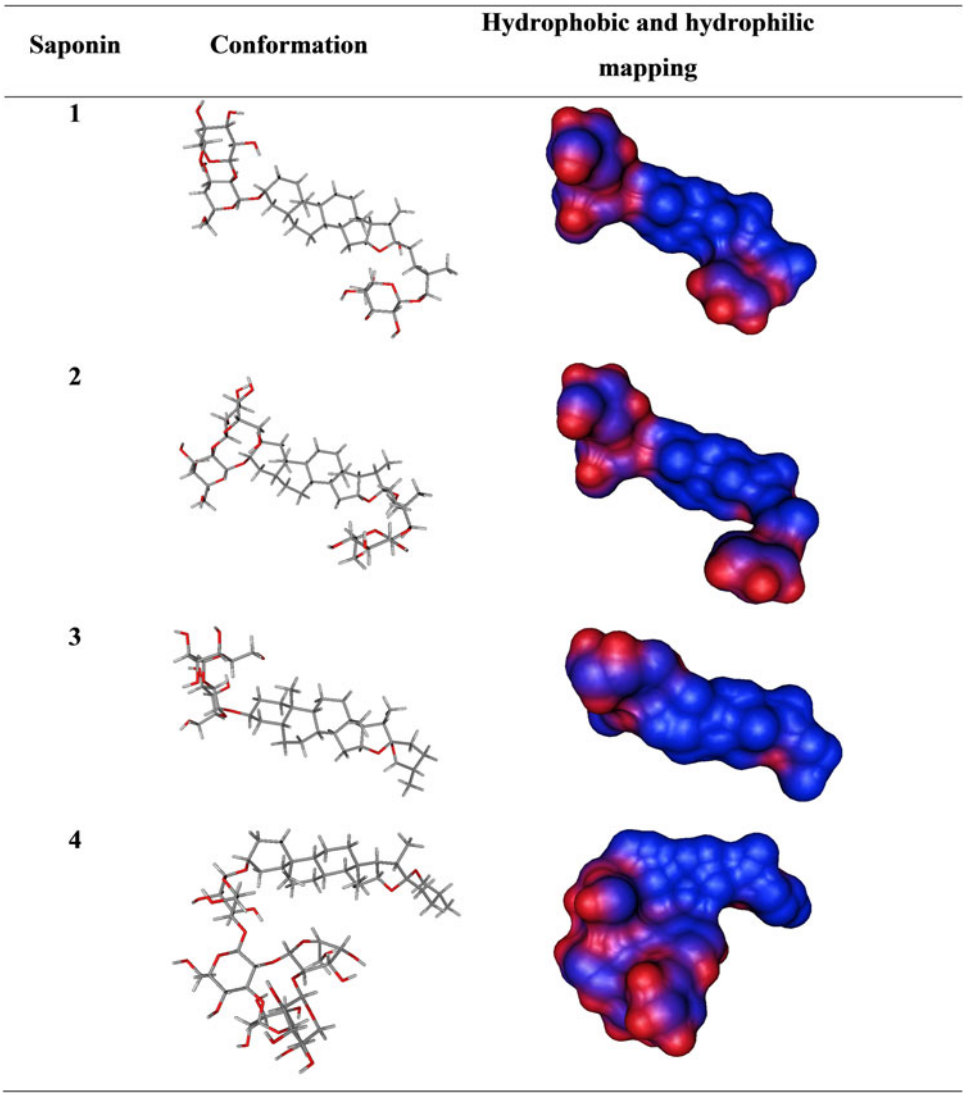


**Fig. 3** Lowest energy conformers of saponins **1**–**4** (*left panel*). Hydrophobic (*blue*) and hydrophilic (*red*) mappings of the lowest energy conformers **1**–**4** (*right panel*) (Color figure online)

the four molecules, we rigidly aligned the local minima best representing each saponin **1**–**4** based on the steroid ring (Fig. 4). The results showed that the lowest energy-minimized structures of the inactive saponins **1** and **2** possessing the common sugar chain β-D-glucopyranosyl-(1 → 2)-*O*-β-D-galactopyranoside, exhibited a common orientation of their sugar moieties with respect to the steroidal plane. In this orientation, the β-D-galactose unit (green) attached to C-3 of the aglycone was roughly in the same plane as the aglycone. A dissimilar orientation of the sugar chain with respect to the steroidal aglycone was noticed upon close inspection of the lowest-energy minimized structure of cytotoxic saponins **3** and **4**. Therein, the β-D-galactose moiety (blue) attached to the aglycone adopted a conformation that is vertical to the steroidal spirostan plane. Even though the sugar moieties of local minima of saponins **3** and **4** failed to align together due to the presence of a different sugar chain at C-3 of aglycone, the vertical orientation of the galactose moiety with respect to the steroidal plane remained intact. Such dissimilarity in orientation of the sugar chain between the pair of saponins **1**, **2** and that of **3**, **4** could be partly attributed to the substitution of the furostan aglycone in **1** and **2** with the spirostan aglycone in **3** and **4**. With regard to this result, it can be concluded that the three dimensional orientation of the galactose moiety that is directly attached to the spirostan aglycone of cytotoxic saponins **3** and **4** contributes to their activity and is of importance to their mode of action. Interestingly, a correlation between spatial geometry and biological activity was previously reported (Labrada *et al.*, 2011; Mimaki *et al.*, 2001). Therefore, it can be concluded that variations in biological activity of saponins **1**–**4** are influenced by their spatial parameters.

To further assess the importance of the spirostanol system for cytotoxic activity, flexible alignment was employed in addition to rigid alignment. Flexible alignment is an application for flexibly aligning small molecules. It is a stochastic search procedure that accepts as input a collection of small

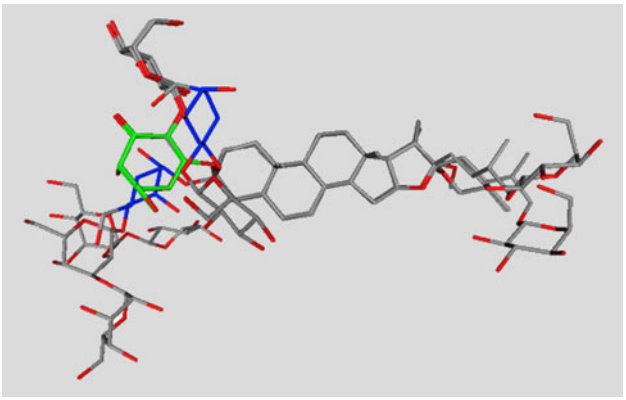

**Fig. 4** Rigid alignment of the molecular geometries of the most stable conformers of saponins **1**–**4**. β-D-galactose unit attached to C-3 of the aglycone is shown in *green* for saponins **1**, **2** and in *blue* for saponins **3**, **4** (Color figure online)

molecules with 3D coordinates and computes a collection of alignments by generating conformations through random rotation of bonds (including ring bonds) instead of only Cartesian coordinate perturbation. Each alignment is given a score that quantifies the quality of the alignment in terms of both internal strain and overlap of molecular features. Often, atomic-level details of the structures of pharmaceutically relevant receptors are not available. In such cases, 3D alignment (or superposition) of putative ligands can be used to deduce structural requirements for biological activity. Methodologies based upon 3D alignment for finding biologically active ligands generally make use of the qualitative assumption that if two ligands align well, they will possess similar biological activity (Kearsley, 1990).

After assigning MMFF94 charges to all molecules, flexible alignment was employed to scan and rank overlays of saponins **1**–**4** based on stearic, electrostatic field, hydrophobic areas overlap, hydrogen bond donors, and acceptors overlap. A common feature of the MOE-generated alignments is an almost complete superposition of the spirostan aglycone of the most active saponins **3** and **4** (0.35 Å) (Fig. 5a); however, a deviation (0.87 Å) is observed at C-3 of the spirostan aglycone, which may indicate the reason behind the slight difference in the cytotoxicity of saponins **3** and **4**.

By the same methodology, saponin **1** was taken as a representative example of the inactive saponin and was subjected to flexible alignment along with **3** and **4**. Saponin **1** (Fig. 5b) was flexibly aligned in a different manner when compared to the congruous alignment of active saponins **3** and **4**, explaining why such a compound was void of antitumor activity. This further proves that the steroid spirostan conjugate of **3** and **4** could be an important factor behind their significant cytotoxicity.

Hydrophobic interactions are the primary driving force in protein–ligand binding and protein folding (Horton and Lewis, 1992; Sarkar and Kellogg, 2010). Recent studies demonstrated that saponin-induced autophagy is governed by protein–ligand interactions through their association with suppression of Akt and ERK1/2 proteins (Dou *et al.*, 2001; Ellington *et al.*, 2006; Tong *et al.*, 2011). Therefore, the construction of hydrophobic mappings for compounds **1**–**4** (Fig. 3) allows us to utilize the spatial conformations of molecules in examining the similarity and dissimilarity in the electronic binding characteristics of their surfaces to possible biological receptors. It can be noted that the presence of the 26-*O*- β-D glucose moiety in **1** and **2** resulted in a different distributions of hydrophilic regions. Comparison of the hydrophobic mappings of **1**–**4** indicated that hydrophilic regions are distributed on both sides (C-3 and C-26 glycoside chains) of saponins **1** and **2**, with a hydrophobic region occupying the agylcone. On the other hand, similarly cytotoxic saponins **3** and **4** share a common one-sided hydrophilic surface distribution located on C-3 of the aglycone owing to the presence of the spirostan ring. This insightful information is important in elucidating the

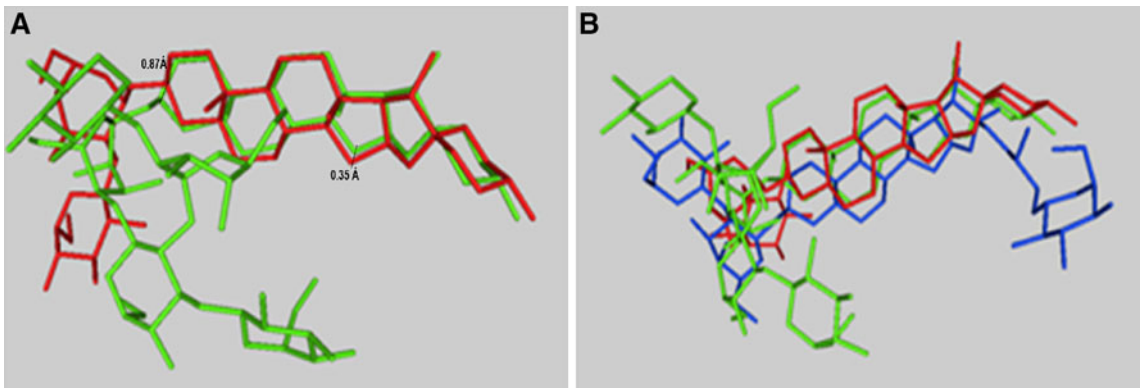


**Fig. 5** **a** Flexible alignments of the most active saponins: **3** (*in red*), **4** (*in green*). **b** Flexible alignments of the inactive saponin **1** (*in blue*) and active saponins **3** (*in red*), **4** (*in green*) (Color figure online)

preferred binding mode of saponins **3** and **4** to complementary amino acid residues of biological receptors.

## Conclusion

Analysis of geometric characteristics by molecular modeling demonstrated their direct influence on biological activity. Our study demonstrated a dissimilar spatial conformation adopted by the 3-*O*- β-D galactosyl moiety of both spirostan and furostan aglycones. Hydrophobic mappings and flexible alignment of the lowest energy conformations of saponins **1**–**4** indicated that biological activity of saponins **3** and **4** could also be attributed to the presence of the spirostan aglycone. Thus, this report represents the first study rationalizing the cytotoxicity of the spirostan aglycone both experimentally and theoretically and is thus important for future SAR studies that might bring out information concerning the apoptotic mechanism of action of saponins.

## Experimental

### General

Optical rotations were determined in MeOH with a Perkin-Elmer 241 polarimeter. $^{1}H$ and $^{13}C$ NMR spectra were recorded in pyridine-$d_5$ on a Bruker DRX-500 at 500 and 125 MHz, respectively, and 2D-NMR experiments were performed using standard Bruker microprograms. ESI–MS and high resolution MS were recorded on Micromass Q-TOF micro instrument (Manchester, UK) with an electrospray source. The samples were introduced by infusion in a solution of MeOH (5 μl/min). TLC was carried out on pre-coated silica gel 60 $F_{254}$ (Merck), and spots were visualized by spraying with 50 % $H_2SO_4$. Kieselgel 60 (63–200 μm, Merck) and Lichroprep RP-18 (40–63 μm, Merck) were used for CC.

### Plant material

The leaves of *Y. de-smetiana* Baker were collected in May 2010 from El-Orman Public Botanical Garden, Giza, Egypt. The plant was identified by Dr. Thérèse Labib, senior specialist of plant identification at El-Orman Public Botanical Garden. A voucher Herbarium specimen (H.M.G. 38, 2010) was deposited in the Herbal Medicinal Garden of Helwan University, Egypt.

### Extraction and isolation

The air dried powdered leaves of *Y. de-smetiana* (1 kg) were extracted three times with MeOH to obtain a concentrated extract (170 g). The methanol extract was suspended in MeOH (350 ml) and precipitated by addition of a large excess of $Me_2CO$ (2 l). The resulting precipitate was filtered and dried to give (75 g) of crude saponin mixture. This mixture was passed through a porous polymer gel column (Mitsubishi Diaion HP-20), eluted with $H_2O$ then MeOH: $H_2O$ (50: 50 and 75: 25) and finally 100 % MeOH. Saponins of fractions eluted with MeOH: $H_2O$ (50: 50) (5 g) were purified by silica gel CC using a gradient of $CHCl_3$: MeOH (80: 20 to 70: 30) to give 69 fractions. Fractions 31–38 (146 mg) were chromatographed successively on silica gel column eluted with $CHCl_3$: MeOH (80: 20 to 75: 25) then by preparative TLC eluted with $CHCl_3$–MeOH–$H_2O$ (70:30:5) to yield pure saponins **1** (12 mg) and **2** (10 mg). Saponins of fractions eluted with 100 % MeOH (1 g) were subjected to silica gel column eluted with $CHCl_3$: MeOH (90: 10 to 78: 22) to afford pure saponins **3** (23 mg) and **4** (20 mg).

### Saponin **4**

White amorphous powder; $[\alpha]_D^{21}$–32.4 (c 0.1, MeOH); $^{1}H$ NMR of the aglycone moiety ($C_5D_5N$):

$\delta$ 4.53 (1H, q, $J = 6.7$ Hz, H-16), 3.89 (1H, m, H-3), 3.58 (1H, m, H-26a), 3.49 (1H, t, $J = 10.9$ Hz, H-26b), 0.47 (1H, td, $J = 12.0$, 3.7 Hz, H-5), 0.61 (3H, s, Me-19), 0.67 (3H, d, $J = 5.6$ Hz, Me-27), 0.80 (3H, s, Me-18), 1.12 (3H, d, $J = 7.0$ Hz, Me-21); $^{13}C$ NMR of the aglycone moiety ($C_5D_5N$):

$\delta$ 36.9 (C-1), 29.7 (C-2), 77.3 (C-3), 34.6 (C-4), 54.1 (C-5), 28.7 (C-6), 32.2 (C-7), 35.0 (C-8), 44.4 (C-9), 35.6 (C-10), 21.0 (C-11), 39.9 (C-12), 40.5 (C-13), 56.2 (C-14), 31.9 (C-15), 81.2 (C-16), 62.8 (C-17), 16.4 (C-18), 12.1 (C-19), 41.7 (C-20), 14.8 (C-21), 109.0 (C-22), 31.6 (C-23), 29.0 (C-24), 30.4 (C-25), 66.8 (C-26), 17.1 (C-27). $^{1}H$ NMR of the sugar moiety ($C_5D_5N$): $\delta$ 4.86 (d, $J = 7.8$ Hz, H-$1_{gal}$), 4.38 (dd, $J = 9.2$, 7.6 Hz, H-$2_{gal}$), 4.08 (m, H-$3_{gal}$), 4.58 (dd, $J = 4.0$, 2.6 Hz, H-$4_{gal}$), 4.07 (m, H-$5_{gal}$), 4.18 (m, H-$6_{gal}$), 4.67 (m, H-$6_{gal}$), 5.13 (d, $J = 7.9$ Hz, H-$1_{glc'}$), 4.34 (t, $J = 8.4$ Hz, H-$2_{glc'}$), 4.14 (dd, $J = 8.8$, 8.4 Hz, H-$3_{glc'}$), 4.12 (t, $J = 9.0$ Hz, H-$4_{glc'}$), 3.82 (m, H-$5_{glc'}$), 4.01 (dd, $J = 11.0$, 5.0 Hz, H-$6_{glc'}$), 4.47 (brd, $J = 10.8$ Hz, H-$6_{glc'}$), 5.20 (d, $J = 7.8$ Hz, H-$1_{glc''}$), 4.02 (dd, $J = 8.9$, 8.0 Hz, H-$2_{glc''}$), 4.13 (m, H-$3_{glc''}$), 4.08 (t, $J = 9.2$ Hz, H-$4_{glc''}$), 3.82 (m, H-$5_{glc''}$), 4.22 (dd, $J = 10.8$, 5.2 Hz, H-$6_{glc''}$), 4.53 (dd, $J = 11.0$, 7.1 Hz, H-$6_{glc''}$), 5.55 (d, $J = 6.8$ Hz, H-$1_{gal'}$), 4.07 (dd, $J = 8.0$, 7.0 Hz, H-$2_{gal'}$), 3.82 (m, H-$3_{gal'}$), 4.04 (d, $J = 2.5$ Hz, H-$4_{gal'}$), 4.00 (m, H-$5_{gal'}$), 4.28 (dd, $J = 11.0$, 7.5 Hz, H-$6_{gal'}$), 4.47 (brd, $J = 10.8$ Hz, H-$6_{gal'}$), 5.09 (d, $J = 7.4$ Hz, H-$1_{xyl}$), 3.92 (t, $J = 8.6$ Hz, H-$2_{xyl}$), 4.05 (t, $J = 8.5$ Hz, H-$3_{xyl}$), 4.08 (m, H-$4_{xyl}$), 3.58 (m, H-$5_{xyl}$), 4.18 (dd, $J = 10.2$, 5.0 Hz, H-$5_{xyl}$).

$^{13}$C NMR of the sugar moiety ($C_5D_5N$): $\delta$ 102.2 (C-$1_{gal}$), 72.9 (C-$2_{gal}$), 75.3 (C-$3_{gal}$), 79.7 (C-$4_{gal}$), 75.3 (C-$5_{gal}$), 60.4 (C-$6_{gal}$), 104.6 (C-$1_{glc'}$), 80.6 (C-$2_{glc'}$), 88.3 (C-$3_{glc'}$), 71.4 (C-$4_{glc'}$), 77.9 (C-$5_{glc'}$), 62.8 (C-$6_{glc'}$), 104.3 (C-$1_{glc''}$), 75.2 (C-$2_{glc''}$), 78.2 (C-$3_{glc''}$), 70.5 (C-$4_{glc''}$), 77.2 (C-$5_{glc''}$), 62.1 (C-$6_{glc''}$), 103.8 (C-$1_{gal'}$), 86.6 (C-$2_{gal'}$), 70.6 (C-$3_{gal'}$), 74.8 (C-$4_{gal'}$), 78.4 (C-$5_{gal'}$), 61.8 (C-$6_{gal'}$), 105.9 (C-$1_{xyl}$), 75.2 (C-$2_{xyl}$), 77.5 (C-$3_{xyl}$), 68.8 (C-$4_{xyl}$), 66.6 (C-$5_{xyl}$). High-resolution ESI–MS$^+$ $[M + Na]^+$: *m/z* 1219.5735 (calc. 1219.5724, $C_{56}H_{92}O_{27}Na$); ESI–MS $^+$: 1088.5 $[M + Na\text{-xylosyl}]^+$, 925.5 $[M + Na\text{-galactosyl}]^+$, 763.4 $[M + Na\text{-glucosyl}]^+$, 601.4 $[M + Na\text{-glucosyl}]^+$.

## Acid hydrolysis

The crude saponin mixture (100 mg) was refluxed with 10 ml of 2 N HCl at 100 °C for 5 h. After cooling, the reaction was extracted with $CHCl_3$ to remove aglycones. The acid aqueous layer was neutralized with 1 N KOH and evaporated. Three sugars were identified and compared with authentic samples by TLC using solvent MeCOEt–iso-PrOH–$Me_2CO$–$H_2O$ (20:10:7:6) as glucose, galactose, and xylose. The purification of these sugars was achieved by prep. TLC using Kieselgel 60 plates which were eluted three times with solv., $CHCl_3$–MeOH–$H_2O$ (70:30:1) to afford D-glucose ($R_f$ 0.26, $[\alpha]_D^{21}$ +53; $H_2O$), D-galactose ($R_f$ 0.27, $[\alpha]_D^{21}$ +56; $H_2O$), D-xylose ($R_f$ 0.48, $[\alpha]_D^{21}$ +15; $H_2O$).

## Cytotoxicity assays

Cell viability was assessed by the mitochondrial dependent reduction of yellow MTT (3-(4,5-dimethylthiazol-2-yl)-2,5-diphenyl tetrazolium bromide) to purple formazan (Mosmann, 1983). All the following procedures were done in a sterile area using a Laminar flow cabinet biosafety class II level (Baker, SG403INT, Sanford, ME, USA). Cells were suspended in RPMI 1640 medium [(for HePG2-MCF7 and HCT116–DMEM for A549)], 1 % antibiotic–antimycotic mixture (10,000 µg/ml Potassium Penicillin, 10,000 µg/ml Streptomycin Sulfate, and 25 µg/ml Amphotericin B), and 1 % L-glutamine at 37 °C under 5 % $CO_2$. Cells were batch cultured for 10 days, then seeded at a concentration of $10 \times 10^3$ cells/well in fresh complete growth medium in 96-well micro titer plastic plates at 37 °C for 24 h under 5 % $CO_2$ using a water jacketed carbon dioxide incubator (Sheldon, TC2323, Cornelius, OR, USA). Media was aspirated, fresh medium (without serum) was added, and cells were incubated either alone (negative control) or with different concentrations of sample to give a final concentration of (100–50–25–12.5–6.25–3.125–0.78 and 1.56 µM). After 48 h of incubation, medium was aspirated, 40 µl MTT salt (2.5 µg/ml) was added to each well, and incubated for further four hours at 37 °C under 5 % $CO_2$. To stop the reaction and to dissolve the formed crystals, 200 µl of 10 % Sodium dodecyl sulfate (SDS) in deionized water was added to each well and incubated overnight at 37 °C. A positive control composed of 100 µg/ml was used as a known cytotoxic natural agent, which gives 100 % lethality under the same conditions (Thabrew *et al.*, 1997).The absorbance was then measured using a microplate multi-well reader (Bio-Rad Laboratories Inc., model 3350, Hercules, California, USA) at 595 nm and a reference wavelength of 620 nm. A statistical significance was tested between samples and negative control (cells with vehicle) using independent *t* test by SPSS 11 program. DMSO is the vehicle used for dissolution of plant extracts, and its final concentration on the cells was less than 0.2 %. The percentage of change in viability was calculated according to the formula: (Reading of extract/Reading of negative control) $-1 \times 100$. A probit analysis was carried for IC50 and IC90 determination using SPSS 11 program.

## Molecular modeling calculations

### *Energy minimization*

This was performed by use of the Merck forcefield (MMFF94) as implemented in MOE 2008.10. program (Chemical Computing Group Inc., Montreal, Canada). This energy minimization methodology is capable of calculating constrained geometries through the use of chiral, distance, angle, and dihedral restraints (Halgren, 1996). Hydrogen atoms and lone pairs were added to each molecule. Energy minimization was terminated when the root mean square gradient fell below 0.05. Force field partial charges were calculated prior to energy minimization.

### *Flexible alignment*

Using MOE/MMFF94, 200 conformers of each compound were generated and minimized with a distance-dependent dielectric model. Each resulting conformation was checked to determine if it had already been generated by comparing all atom positions using a predefined root-mean-square (RMS) tolerance (0.5 Å). The procedure was terminated when the number of failures to find new conformations exceeded 20 in a row, a stringent criterion. Conformations with energies over 10 kcal/mol above the respective minima were rejected. Chirality was preserved using signed volume restraints on all chiral centers. All open chain bonds and flexible ring bonds were set to random dihedral angles. The alignment mode was chosen as flexible. In the calculations, a bias of $\sim 30°$ was selected, which means that dihedral angles were rotated by random angle with a sum-of-gaussians distribution with peaks at multiples of

30°. From the top scoring superpositions obtained, only one was consistent with the structure–activity relationships of the aligned saponins, and this was subjected to a more refined searching using MOE/flexible alignment module.

**Acknowledgments** The authors are grateful to Dr. Khaled Mohamed, Bioassay-Cell Culture Laboratory, National Research Center- Cairo, Egypt, for carrying the antitumor activity.

## References

Agrawal PK (2003) Spectral assignments and reference data. Magn Reson Chem 41:965–968

Agrawal PK, Jain DC, Gupta RK, Thakur RS (1985) Carbon-13 NMR spectroscopy of steroidal sapogenins and steroidal saponins. Phytochemistry 24:2479–2496

Ali MS, Sharma GC, Asplund RO, Nevins MP, Garb S (1978) Isolation of antitumor polysaccharide fractions from *Yucca glauca Nutt*. (Lilliaceae). Growth 42:213–223

Anthony NB, Balog JM, Staudinger FB, Walker RD, Huff WE (1994) Environmental variability and incidence of ascites. Poult Sci 73:801–809

Bahuguna S, Sati OP (1990) Spirostanol saponins from *Yucca aloifolia* rhizomes. Phytochemistry 29:342–343

Balestrieri C, Piacente S, Pizza C, Montoro P, Oleszek W, Visciano V, Balestrieri ML (2006) Relative effects of phenolic constituents from *Yucca schidigera* Roezl. bark on kaposi's sarcoma cell proliferation, migration, and PAF synthesis. Biochempharmacol 71:1479–1487

Balog JM, Anthony NB, Wall CV, Walker RD, Rath NC, Huff WE (1994) Blood variables, ascites scores and body and organ weights. Poult Sci 73:810–816

Cheeke PR (2000) Actual and potential applications of *Yucca schidigera* and *Quillaia saponaria* saponins in human and animal nutrition. J Anim Sci 77:1–10

Diab Y, Ioannou E, Emam A, Vagias C, Roussis V (2012) Desmettianosides A and B, bidesmosidic furostanol saponins with molluscicidal activity from *Yucca desmettiana*. Steroids 77:686–690

Dou DQ, Zhang YW, Zhang L, Chen YJ, Yao XS (2001) The inhibitory effects of ginsenosides on protein tyrosine kinase activated by hypoxia/reoxygenation in cultured human umbilical vein endothelial cells. Planta Med 67:19–23

Dragalin IP, Kintia PK (1975) Steroidal saponins of *Yucca filamentosa*: yuccoside C and protoyuccoside C. Phytochemistry 14: 1817–1820

Ellington AA, Berhowl MA, Singletary KW (2006) Inhibition of Akt signaling and enhanced ERK1/2 activity are involved in induction of macroautophagy by triterpenoid B-group soyasaponins in colon cancer cells. Carcinogenesis 27:298–306

Eskander J, Lavaud C, Harakat D (2010) Steroidal saponins from the leaves of *Agave macroacantha*. Fitoterapia 81:371–374

Eskander J, Lavaud C, Harakat D (2011) Steroidal saponins from the leaves of *Beaucarnea recurvata*. Phytochemistry 72:946–951

Gonzalez AG, Hernandez JC, Leon F, Padron JI, Estevez F, Quintana J, Bermejo J (2003) Steroidal saponins from the bark of *Dracaena draco* and their cytotoxic activities. J Nat Prod 66:793–798

Halgren TA (1996) Merck molecular force field. I. Basis, form, scope, parameterization, and performance of MMFF94. J Comp Chem 17:490–519

Horton N, Lewis M (1992) Calculation of the free energy of association for protein complexes. Prot Sci 1:169–181

Hostettmann KA, Marston A (1995) Saponins chemistry and pharmacology of natural products. Cambridge University Press, Cambridge

Jin Y, Kuk J, Oh K, Kim Y, Piao X, Park R (2007) A new steroidal saponin, yuccalan, from the leaves of *Yucca smalliana*. Arch Pharm Res 30:543–546

Kearsley S (1990) An alternative method for the alignment of molecular structures: maximizing electrostatic and steric overlap. Tetrahedron Comput Methodol 3:615–633

Labrada KP, Brouard I, Morera C, Estevez F, Bermejo J, Rivera DG (2011) 'Click' synthesis of triazole- based spirostan saponin analogs. Tetrahedron 67:7713–7727

Liu MJ, Wang Z, Ju Y, Zhou JB, Wang Y, Wong RNS (2004) The mitotic-arresting and apoptosis-inducing effects of diosgenyl saponins on human leukemia cell lines. Biol Pharm Bull 27:1059–1065

Mahato SB, Ganguly AN, Sahu NP (1982) Steroid saponins. Phytochemistry 21:959–978

Mimaki Y, Yokosuka A, Kuroda M, Sashida Y (2001) Cytotoxic activities and structure-cytotoxic relationships of steroidal saponins. Biol Pharm Bull 24:1286–1289

Mosmann T (1983) Rapid colorimetric assays for cellular growth and survival: application to proliferation and cytotoxicity assays. J Immunol Methods 65:55–63

Nakano K, Yamasaki T, Imamura Y, Murakami K, Takaishi Y, Tomimatsu T (1989) The steroidal glycosides from the stem of *Yucca gloriosa*. Phytochemistry 28:1215–1217

Oleszek W, Sitek M, Stochmal A, Piacente S, Pizza C, Cheeke P (2001) Steroidal saponins of *Yucca schidigera* Roezl. J Agric Food Chem 49:4392–4396

Piacente S, Pizza C, Oleszek W (2005) Saponins and phenolics of *Yucca schidigera* Roezl: chemistry and bioactivity. Phytochem Rev 4:177–190

Sarkar A, Kellogg GE (2010) Hydrophobicity-shake flasks, protein folding and drug discovery. Curr Top Med Chem 10:67–83

Skhirtladze A, Plaza A, Montoro P, Benidze M, Kemetelidze E, Pizza C, Piacente S (2006) Furostanol saponins from *Yucca gloriosa* L. rhizomes. Biochem Syst Ecol 34:809–814

Thabrew MI, Hughes RD, McFarlane IG (1997) Screening of hepatoprotective plant components using a HepG2 cell cytotoxicity assay. J Pharm Pharmacol 49:1132–1135

Tong QY, Qing Y, Shu D, He Y, Zhao YL, Li Y, Wang ZL, Zhang SY, Xing ZH, Xu C, Wei YQ, Huang W, Wu XH (2011) Deltonin, a steroidal saponin, inhibits colon cancer cell growth in vitro and tumor growth in vivo via induction of apoptosis and antiangiogenesis. Cell Physiol Biochem 27:233–242

Trouillas P, Corbiere C, Liagre B, Duroux JL, Beneytout JL (2005) Structure-function relationship for saponin effects on cell cycle arrest and apoptosis in the human 1547 osteosarcoma cells: a molecular modelling approach of natural molecules structurally close to diosgenin. Bioorg Med Chem 13:1141–1149

Yuen-Nei Cheung J, Chik-Ying Ong R, Suen YK, Ooi V, Nai-Ching Wong H, Chung-Wai Mak T, Fung KP, Yu B, Kong SK (2005) Polyphyllin D is a potent apoptosis inducer in drug-resistant HepG2 cells. Cancer Lett 217:203–211

Zhang Y, Zhang Y-J, Jacob MR, Li X, Yang C (2008) Steroidal saponins from the stem of *Yucca elephantipes*. Phytochemistry 69:264–270